Measurements of branching fraction ratios and *CP* asymmetries in $B^\pm \to D_{CP} K^\pm$ decays in hadron collisions

T. Aaltonen,[24] J. Adelman,[14] B. Álvarez González,[12,w] S. Amerio,[44b,44a] D. Amidei,[35] A. Anastassov,[39] A. Annovi,[20] J. Antos,[15] G. Apollinari,[18] A. Apresyan,[49] T. Arisawa,[58] A. Artikov,[16] J. Asaadi,[54] W. Ashmanskas,[18] A. Attal,[4] A. Aurisano,[54] F. Azfar,[43] W. Badgett,[18] A. Barbaro-Galtieri,[29] V. E. Barnes,[49] B. A. Barnett,[26] P. Barria,[47c,47a] P. Bartos,[15] G. Bauer,[33] P.-H. Beauchemin,[34] F. Bedeschi,[47a] D. Beecher,[31] S. Behari,[26] G. Bellettini,[47b,47a] J. Bellinger,[60] D. Benjamin,[17] A. Beretvas,[18] A. Bhatti,[51] M. Binkley,[18] D. Bisello,[44b,44a] I. Bizjak,[31,dd] R. E. Blair,[2] C. Blocker,[7] B. Blumenfeld,[26] A. Bocci,[17] A. Bodek,[50] V. Boisvert,[50] D. Bortoletto,[49] J. Boudreau,[48] A. Boveia,[11] B. Brau,[11,b] A. Bridgeman,[25] L. Brigliadori,[6b,6a] C. Bromberg,[36] E. Brubaker,[14] J. Budagov,[16] H. S. Budd,[50] S. Budd,[25] K. Burkett,[18] G. Busetto,[44b,44a] P. Bussey,[22] A. Buzatu,[34] K. L. Byrum,[2] S. Cabrera,[17,y] C. Calancha,[32] S. Camarda,[4] M. Campanelli,[31] M. Campbell,[35] F. Canelli,[14,18] A. Canepa,[46] B. Carls,[25] D. Carlsmith,[60] R. Carosi,[47a] S. Carrillo,[19,o] S. Carron,[18] B. Casal,[12] M. Casarsa,[18] A. Castro,[6b,6a] P. Catastini,[47c,47a] D. Cauz,[55a] V. Cavaliere,[47c,47a] M. Cavalli-Sforza,[4] A. Cerri,[29] L. Cerrito,[31,r] S. H. Chang,[28] Y. C. Chen,[1] M. Chertok,[8] G. Chiarelli,[47a] G. Chlachidze,[18] F. Chlebana,[18] K. Cho,[28] D. Chokheli,[16] J. P. Chou,[23] K. Chung,[18,p] W. H. Chung,[60] Y. S. Chung,[50] T. Chwalek,[27] C. I. Ciobanu,[45] M. A. Ciocci,[47c,47a] A. Clark,[21] D. Clark,[7] G. Compostella,[44a] M. E. Convery,[18] J. Conway,[8] M. Corbo,[45] M. Cordelli,[20] C. A. Cox,[8] D. J. Cox,[8] F. Crescioli,[47b,47a] C. Cuenca Almenar,[61] J. Cuevas,[12,w] R. Culbertson,[18] J. C. Cully,[35] D. Dagenhart,[18] M. Datta,[18] T. Davies,[22] P. de Barbaro,[50] S. De Cecco,[52a] A. Deisher,[29] G. De Lorenzo,[4] M. Dell'Orso,[47b,47a] C. Deluca,[4] L. Demortier,[51] J. Deng,[17,g] M. Deninno,[6a] M. d'Errico,[44b,44a] A. Di Canto,[47b,47a] G. P. di Giovanni,[45] B. Di Ruzza,[47a] J. R. Dittmann,[5] M. D'Onofrio,[4] S. Donati,[47b,47a] P. Dong,[18] T. Dorigo,[44a] S. Dube,[53] K. Ebina,[58] A. Elagin,[54] R. Erbacher,[8] D. Errede,[25] S. Errede,[25] N. Ershaidat,[45,cc] R. Eusebi,[54] H. C. Fang,[29] S. Farrington,[43] W. T. Fedorko,[14] R. G. Feild,[61] M. Feindt,[27] J. P. Fernandez,[32] C. Ferrazza,[47d,47a] R. Field,[19] G. Flanagan,[49,t] R. Forrest,[8] M. J. Frank,[5] M. Franklin,[23] J. C. Freeman,[18] I. Furic,[19] M. Gallinaro,[51] J. Galyardt,[13] F. Garberson,[11] J. E. Garcia,[21] A. F. Garfinkel,[49] P. Garosi,[47c,47a] H. Gerberich,[25] D. Gerdes,[35] A. Gessler,[27] S. Giagu,[52b,52a] V. Giakoumopoulou,[3] P. Giannetti,[47a] K. Gibson,[48] J. L. Gimmell,[50] C. M. Ginsburg,[18] N. Giokaris,[3] M. Giordani,[55b,55a] P. Giromini,[20] M. Giunta,[47a] G. Giurgiu,[26] V. Glagolev,[16] D. Glenzinski,[18] M. Gold,[38] N. Goldschmidt,[19] A. Golossanov,[18] G. Gomez,[12] G. Gomez-Ceballos,[33] M. Goncharov,[33] O. González,[32] I. Gorelov,[38] A. T. Goshaw,[17] K. Goulianos,[51] A. Gresele,[44b,44a] S. Grinstein,[4] C. Grosso-Pilcher,[14] R. C. Group,[18] U. Grundler,[25] J. Guimaraes da Costa,[23] Z. Gunay-Unalan,[36] C. Haber,[29] S. R. Hahn,[18] E. Halkiadakis,[53] B.-Y. Han,[50] J. Y. Han,[50] F. Happacher,[20] K. Hara,[56] D. Hare,[53] M. Hare,[57] R. F. Harr,[59] M. Hartz,[48] K. Hatakeyama,[5] C. Hays,[43] M. Heck,[27] J. Heinrich,[46] M. Herndon,[60] J. Heuser,[27] S. Hewamanage,[5] D. Hidas,[53] C. S. Hill,[11,d] D. Hirschbuehl,[27] A. Hocker,[18] S. Hou,[1] M. Houlden,[30] S.-C. Hsu,[29] R. E. Hughes,[40] M. Hurwitz,[14] U. Husemann,[61] M. Hussein,[36] J. Huston,[36] J. Incandela,[11] G. Introzzi,[47a] M. Iori,[52b,52a] A. Ivanov,[8,q] E. James,[18] D. Jang,[13] B. Jayatilaka,[17] E. J. Jeon,[28] M. K. Jha,[6a] S. Jindariani,[18] W. Johnson,[8] M. Jones,[49] K. K. Joo,[28] S. Y. Jun,[13] J. E. Jung,[28] T. R. Junk,[18] T. Kamon,[54] D. Kar,[19] P. E. Karchin,[59] Y. Kato,[42,n] R. Kephart,[18] W. Ketchum,[14] J. Keung,[46] V. Khotilovich,[54] B. Kilminster,[18] D. H. Kim,[28] H. S. Kim,[28] H. W. Kim,[28] J. E. Kim,[28] M. J. Kim,[20] S. B. Kim,[28] S. H. Kim,[56] Y. K. Kim,[14] N. Kimura,[58] L. Kirsch,[7] S. Klimenko,[19] K. Kondo,[58] D. J. Kong,[28] J. Konigsberg,[19] A. Korytov,[19] A. V. Kotwal,[17] M. Kreps,[27] J. Kroll,[46] D. Krop,[14] N. Krumnack,[5] M. Kruse,[17] V. Krutelyov,[11] T. Kuhr,[27] N. P. Kulkarni,[59] M. Kurata,[56] S. Kwang,[14] A. T. Laasanen,[49] S. Lami,[47a] S. Lammel,[18] M. Lancaster,[31] R. L. Lander,[8] K. Lannon,[40,v] A. Lath,[53] G. Latino,[47c,47a] I. Lazzizzera,[44b,44a] T. LeCompte,[2] E. Lee,[54] H. S. Lee,[14] J. S. Lee,[28] S. W. Lee,[54,x] S. Leone,[47a] J. D. Lewis,[18] C.-J. Lin,[29] J. Linacre,[43] M. Lindgren,[18] E. Lipeles,[46] A. Lister,[21] D. O. Litvintsev,[18] C. Liu,[48] T. Liu,[18] N. S. Lockyer,[46] A. Loginov,[61] L. Lovas,[15] D. Lucchesi,[44b,44a] J. Lueck,[27] P. Lujan,[29] P. Lukens,[18] G. Lungu,[51] J. Lys,[29] R. Lysak,[15] D. MacQueen,[34] R. Madrak,[18] K. Maeshima,[18] K. Makhoul,[33] P. Maksimovic,[26] S. Malde,[43] S. Malik,[31] G. Manca,[30,f] A. Manousakis-Katsikakis,[3] F. Margaroli,[49] C. Marino,[27] C. P. Marino,[25] A. Martin,[61] V. Martin,[22,l] M. Martínez,[4] R. Martínez-Ballarín,[32] P. Mastrandrea,[52a] M. Mathis,[26] M. E. Mattson,[59] P. Mazzanti,[6a] K. S. McFarland,[50] P. McIntyre,[54] R. McNulty,[30,k] A. Mehta,[30] P. Mehtala,[24] A. Menzione,[47a] C. Mesropian,[51] T. Miao,[18] D. Mietlicki,[35] N. Miladinovic,[7] R. Miller,[36] C. Mills,[23] M. Milnik,[27] A. Mitra,[1] G. Mitselmakher,[19] H. Miyake,[56] S. Moed,[23] N. Moggi,[6a] M. N. Mondragon,[18,o] C. S. Moon,[28] R. Moore,[18] M. J. Morello,[47a] J. Morlock,[27] P. Movilla Fernandez,[18] J. Mülmenstädt,[29] A. Mukherjee,[18] Th. Muller,[27] P. Murat,[18] M. Mussini,[6b,6a] J. Nachtman,[18,p] Y. Nagai,[56] J. Naganoma,[56] K. Nakamura,[56] I. Nakano,[41] A. Napier,[57] J. Nett,[60] C. Neu,[46,aa] M. S. Neubauer,[25] S. Neubauer,[27] J. Nielsen,[29,h] L. Nodulman,[2] M. Norman,[10] O. Norniella,[25] E. Nurse,[31] L. Oakes,[43] S. H. Oh,[17] Y. D. Oh,[28] I. Oksuzian,[19] T. Okusawa,[42] R. Orava,[24] K. Osterberg,[24] S. Pagan Griso,[44b,44a]

C. Pagliarone,[55a] E. Palencia,[18] V. Papadimitriou,[18] A. Papaikonomou,[27] A. A. Paramanov,[2] B. Parks,[40] S. Pashapour,[34] J. Patrick,[18] G. Pauletta,[55b,55a] M. Paulini,[13] C. Paus,[33] T. Peiffer,[27] D. E. Pellett,[8] A. Penzo,[55a] T. J. Phillips,[17] G. Piacentino,[47a] E. Pianori,[46] L. Pinera,[19] K. Pitts,[25] C. Plager,[9] L. Pondrom,[60] K. Potamianos,[49] O. Poukhov,[16,a] F. Prokoshin,[16,z] A. Pronko,[18] F. Ptohos,[18,j] E. Pueschel,[13] G. Punzi,[47b,47a] J. Pursley,[60] J. Rademacker,[43,d] A. Rahaman,[48] V. Ramakrishnan,[60] N. Ranjan,[49] I. Redondo,[32] P. Renton,[43] M. Renz,[27] M. Rescigno,[52a] S. Richter,[27] F. Rimondi,[6b,6a] L. Ristori,[47a] A. Robson,[22] T. Rodrigo,[12] T. Rodriguez,[46] E. Rogers,[25] S. Rolli,[57] R. Roser,[18] M. Rossi,[55a] R. Rossin,[11] P. Roy,[34] A. Ruiz,[12] J. Russ,[13] V. Rusu,[18] B. Rutherford,[18] H. Saarikko,[24] A. Safonov,[54] W. K. Sakumoto,[50] L. Santi,[55b,55a] L. Sartori,[47a] K. Sato,[56] A. Savoy-Navarro,[45] P. Schlabach,[18] A. Schmidt,[27] E. E. Schmidt,[18] M. A. Schmidt,[14] M. P. Schmidt,[61,a] M. Schmitt,[39] T. Schwarz,[8] L. Scodellaro,[12] A. Scribano,[47c,47a] F. Scuri,[47a] A. Sedov,[49] S. Seidel,[38] Y. Seiya,[42] A. Semenov,[16] L. Sexton-Kennedy,[18] F. Sforza,[47b,47a] A. Sfyrla,[25] S. Z. Shalhout,[59] T. Shears,[30] P. F. Shepard,[48] M. Shimojima,[56,u] S. Shiraishi,[14] M. Shochet,[14] Y. Shon,[60] I. Shreyber,[37] A. Simonenko,[16] P. Sinervo,[34] A. Sisakyan,[16] A. J. Slaughter,[18] J. Slaunwhite,[40] K. Sliwa,[57] J. R. Smith,[8] F. D. Snider,[18] R. Snihur,[34] A. Soha,[18] S. Somalwar,[53] V. Sorin,[4] P. Squillacioti,[47c,47a] M. Stanitzki,[61] R. St. Denis,[22] B. Stelzer,[34] O. Stelzer-Chilton,[34] D. Stentz,[39] J. Strologas,[38] G. L. Strycker,[35] J. S. Suh,[28] A. Sukhanov,[19] I. Suslov,[16] A. Taffard,[25,g] R. Takashima,[41] Y. Takeuchi,[56] R. Tanaka,[41] J. Tang,[14] M. Tecchio,[35] P. K. Teng,[1] J. Thom,[18,i] J. Thome,[13] G. A. Thompson,[25] E. Thomson,[46] P. Tipton,[61] P. Ttito-Guzmán,[32] S. Tkaczyk,[18] D. Toback,[54] S. Tokar,[15] K. Tollefson,[36] T. Tomura,[56] D. Tonelli,[18] S. Torre,[20] D. Torretta,[18] P. Totaro,[55b,55a] S. Tourneur,[45] M. Trovato,[47d,47a] S.-Y. Tsai,[1] Y. Tu,[46] N. Turini,[47c,47a] F. Ukegawa,[56] S. Uozumi,[28] N. van Remortel,[24,c] A. Varganov,[35] E. Vataga,[47d,47a] F. Vázquez,[19,o] G. Velev,[18] C. Vellidis,[3] M. Vidal,[32] I. Vila,[12] R. Vilar,[12] M. Vogel,[38] I. Volobouev,[29,x] G. Volpi,[47b,47a] P. Wagner,[46] R. G. Wagner,[2] R. L. Wagner,[18] W. Wagner,[27,bb] J. Wagner-Kuhr,[27] T. Wakisaka,[42] R. Wallny,[9] S. M. Wang,[1] A. Warburton,[34] D. Waters,[31] M. Weinberger,[54] J. Weinelt,[27] W. C. Wester III,[18] B. Whitehouse,[57] D. Whiteson,[46,g] A. B. Wicklund,[2] E. Wicklund,[18] S. Wilbur,[14] G. Williams,[34] H. H. Williams,[46] P. Wilson,[18] B. L. Winer,[40] P. Wittich,[18,i] S. Wolbers,[18] C. Wolfe,[14] H. Wolfe,[40] T. Wright,[35] X. Wu,[21] F. Würthwein,[10] A. Yagil,[10] K. Yamamoto,[42] J. Yamaoka,[17] U. K. Yang,[14,s] Y. C. Yang,[28] W. M. Yao,[29] G. P. Yeh,[18] K. Yi,[18,p] J. Yoh,[18] K. Yorita,[58] T. Yoshida,[42,m] G. B. Yu,[17] I. Yu,[28] S. S. Yu,[18] J. C. Yun,[18] A. Zanetti,[55a] Y. Zeng,[17] X. Zhang,[25] Y. Zheng,[9,e] and S. Zucchelli[6b,6a]

(CDF Collaboration)

[1]*Institute of Physics, Academia Sinica, Taipei, Taiwan 11529, Republic of China*
[2]*Argonne National Laboratory, Argonne, Illinois 60439, USA*
[3]*University of Athens, 157 71 Athens, Greece*
[4]*Institut de Fisica d'Altes Energies, Universitat Autonoma de Barcelona, E-08193, Bellaterra (Barcelona), Spain*
[5]*Baylor University, Waco, Texas 76798, USA*
[6a]*Istituto Nazionale di Fisica Nucleare Bologna, I-40127 Bologna, Italy*
[6b]*University of Bologna, I-40127 Bologna, Italy*
[7]*Brandeis University, Waltham, Massachusetts 02254, USA*
[8]*University of California, Davis, Davis, California 95616, USA*
[9]*University of California, Los Angeles, Los Angeles, California 90024, USA*
[10]*University of California, San Diego, La Jolla, California 92093, USA*
[11]*University of California, Santa Barbara, Santa Barbara, California 93106, USA*
[12]*Instituto de Fisica de Cantabria, CSIC-University of Cantabria, 39005 Santander, Spain*
[13]*Carnegie Mellon University, Pittsburgh, Pennsylvania 15213, USA*
[14]*Enrico Fermi Institute, University of Chicago, Chicago, Illinois 60637, USA*
[15]*Comenius University, 842 48 Bratislava, Slovakia;*
Institute of Experimental Physics, 040 01 Kosice, Slovakia
[16]*Joint Institute for Nuclear Research, RU-141980 Dubna, Russia*
[17]*Duke University, Durham, North Carolina 27708, USA*
[18]*Fermi National Accelerator Laboratory, Batavia, Illinois 60510, USA*
[19]*University of Florida, Gainesville, Florida 32611, USA*
[20]*Laboratori Nazionali di Frascati, Istituto Nazionale di Fisica Nucleare, I-00044 Frascati, Italy*
[21]*University of Geneva, CH-1211 Geneva 4, Switzerland*
[22]*Glasgow University, Glasgow G12 8QQ, United Kingdom*
[23]*Harvard University, Cambridge, Massachusetts 02138, USA*
[24]*Division of High Energy Physics, Department of Physics, University of Helsinki and Helsinki Institute of Physics, FIN-00014, Helsinki, Finland*

[25]University of Illinois, Urbana, Illinois 61801, USA

[26]The Johns Hopkins University, Baltimore, Maryland 21218, USA

[27]Institut für Experimentelle Kernphysik, Karlsruhe Institute of Technology, D-76131 Karlsruhe, Germany

[28]Center for High Energy Physics: Kyungpook National University, Daegu 702-701, Korea;

Seoul National University, Seoul 151-742, Korea;

Sungkyunkwan University, Suwon 440-746, Korea;

Korea Institute of Science and Technology Information, Daejeon 305-806, Korea;

Chonnam National University, Gwangju 500-757, Korea;

Chonbuk National University, Jeonju 561-756, Korea

[29]Ernest Orlando Lawrence Berkeley National Laboratory, Berkeley, California 94720, USA

[30]University of Liverpool, Liverpool L69 7ZE, United Kingdom

[31]University College London, London WC1E 6BT, United Kingdom

[32]Centro de Investigaciones Energeticas Medioambientales y Tecnologicas, E-28040 Madrid, Spain

[33]Massachusetts Institute of Technology, Cambridge, Massachusetts 02139, USA

[34]Institute of Particle Physics: McGill University, Montréal, Québec, Canada H3A 2T8;

Simon Fraser University, Burnaby, British Columbia, Canada V5A 1S6;

University of Toronto, Toronto, Ontario, Canada M5S 1A7;

and TRIUMF, Vancouver, British Columbia, Canada V6T 2A3

[35]University of Michigan, Ann Arbor, Michigan 48109, USA

[36]Michigan State University, East Lansing, Michigan 48824, USA

[37]Institution for Theoretical and Experimental Physics, ITEP, Moscow 117259, Russia

[38]University of New Mexico, Albuquerque, New Mexico 87131, USA

[39]Northwestern University, Evanston, Illinois 60208, USA

[40]The Ohio State University, Columbus, Ohio 43210, USA

[41]Okayama University, Okayama 700-8530, Japan

[42]Osaka City University, Osaka 588, Japan

[43]University of Oxford, Oxford OX1 3RH, United Kingdom

[44a]Istituto Nazionale di Fisica Nucleare, Sezione di Padova-Trento, I-35131 Padova, Italy

[44b]University of Padova, I-35131 Padova, Italy

[45]LPNHE, Universite Pierre et Marie Curie/IN2P3-CNRS, UMR7585, Paris, F-75252 France

[46]University of Pennsylvania, Philadelphia, Pennsylvania 19104, USA

[47a]Istituto Nazionale di Fisica Nucleare Pisa, I-56127 Pisa, Italy

[a]Deceased.

[b]Visitor from University of Massachusetts Amherst, Amherst, MA 01003, USA.

[c]Visitor from Universiteit Antwerpen, B-2610 Antwerp, Belgium.

[d]Visitor from University of Bristol, Bristol BS8 1TL, United Kingdom.

[e]Visitor from Chinese Academy of Sciences, Beijing 100864, China.

[f]Visitor from Istituto Nazionale di Fisica Nucleare, Sezione di Cagliari, 09042 Monserrato (Cagliari), Italy.

[g]Visitor from University of California Irvine, Irvine, CA 92697, USA.

[h]Visitor from University of California Santa Cruz, Santa Cruz, CA 95064, USA..

[i]Visitor from Cornell University, Ithaca, NY 14853, USA.

[j]Visitor from University of Cyprus, Nicosia CY-1678, Cyprus.

[k]Visitor from University College Dublin, Dublin 4, Ireland.

[l]Visitor from University of Edinburgh, Edinburgh EH9 3JZ, United Kingdom.

[m]Visitor from University of Fukui, Fukui City, Fukui Prefecture, Japan 910-0017.

[n]Visitor from Kinki University, Higashi-Osaka City, Japan 577-8502.

[o]Visitor from Universidad Iberoamericana, Mexico D.F., Mexico.

[p]Visitor from University of Iowa, Iowa City, IA 52242, USA.

[q]Visitor from Kansas State University, Manhattan, KS 66506, USA.

[r]Visitor from Queen Mary, University of London, London, E1 4NS, England, United Kingdom.

[s]Visitor from University of Manchester, Manchester M13 9PL, England, United Kingdom.

[t]Visitor from Muons, Inc., Batavia, IL 60510, USA.

[u]Visitor from Nagasaki Institute of Applied Science, Nagasaki, Japan.

[v]Visitor from University of Notre Dame, Notre Dame, IN 46556, USA.

[w]Visitor from University de Oviedo, E-33007 Oviedo, Spain.

[x]Visitor from Texas Tech University, Lubbock, TX 79609, USA.

[y]Visitor from IFIC (CSIC-Universitat de Valencia), 56071 Valencia, Spain.

[z]Visitor from Universidad Tecnica Federico Santa Maria, 110v Valparaiso, Chile.

[aa]Visitor from University of Virginia, Charlottesville, VA 22906, USA.

[bb]Visitor from Bergische Universität Wuppertal, 42097 Wuppertal, Germany.

[cc]Visitor from Yarmouk University, Irbid 211-63, Jordan.

[dd]On leave from J. Stefan Institute, Ljubljana, Slovenia.

^{47b}*University of Pisa, I-56127 Pisa, Italy*
^{47c}*University of Siena, , I-56127 Pisa, Italy*
^{47d}*Scuola Normale Superiore, I-56127 Pisa, Italy*
^{48}*University of Pittsburgh, Pittsburgh, Pennsylvania 15260, USA*
^{49}*Purdue University, West Lafayette, Indiana 47907, USA*
^{50}*University of Rochester, Rochester, New York 14627, USA*
^{51}*The Rockefeller University, New York, New York 10021, USA*
^{52a}*Istituto Nazionale di Fisica Nucleare, Sezione di Roma 1, I-00185 Roma, Italy*
^{52b}*Sapienza Università di Roma, I-00185 Roma, Italy*
^{53}*Rutgers University, Piscataway, New Jersey 08855, USA*
^{54}*Texas A&M University, College Station, Texas 77843, USA*
^{55a}*Istituto Nazionale di Fisica Nucleare Trieste/Udine, I-34100 Trieste, I-33100 Udine, Italy*
^{55b}*University of Trieste/Udine, I-33100 Udine, Italy*
^{56}*University of Tsukuba, Tsukuba, Ibaraki 305, Japan*
^{57}*Tufts University, Medford, Massachusetts 02155, USA*
^{58}*Waseda University, Tokyo 169, Japan*
^{59}*Wayne State University, Detroit, Michigan 48201, USA*
^{60}*University of Wisconsin, Madison, Wisconsin 53706, USA*
^{61}*Yale University, New Haven, Connecticut 06520, USA*

We reconstruct $B^{\pm} \to DK^{\pm}$ decays in a data sample collected by the CDF II detector at the Tevatron collider corresponding to 1 fb^{-1} of integrated luminosity. We select decay modes where the D meson decays to either $K^{-}\pi^{+}$ (flavor eigenstate) or $K^{-}K^{+}$, $\pi^{-}\pi^{+}$ (*CP*-even eigenstates), and measure the direct *CP* asymmetry $A_{CP+} = 0.39 \pm 0.17(\text{stat}) \pm 0.04(\text{syst})$, and the double ratio of *CP*-even to flavor eigenstate branching fractions $R_{CP+} = 1.30 \pm 0.24(\text{stat}) \pm 0.12(\text{syst})$. These measurements will improve the determination of the Cabibbo-Kobayashi-Maskawa angle γ. They are performed here for the first time using data from hadron collisions.

The measurement of *CP* asymmetries and branching ratios of $B^{-} \to DK^{-}$ [1] decay modes allows a theoretically clean extraction of the Cabibbo-Kobayashi-Maskawa (CKM) angle $\gamma = \arg(-V_{ud}V_{ub}^{*}/V_{cd}V_{cb}^{*})$, a fundamental parameter of the standard model [2]. In these decays the interference between the tree amplitudes of the $b \to c\bar{u}s$ and $b \to u\bar{c}s$ processes leads to observables that depend on their relative weak phase (γ), their relative strong phase (δ_B), and the magnitude ratio $r_B = |\frac{A(b \to u)}{A(b \to c)}|$. These quantities can all be extracted from data by combining several experimental observables. This can be achieved in several ways, from a variety of D decay channels [3–5].

An accurate knowledge of the value of γ is instrumental in establishing the possible presence of additional non-standard model *CP*-violating phases in higher-order diagrams [6,7]. Its current determination is based on a combination of several $B \to DK$ measurements performed in $e^{+}e^{-}$ collisions at the $\Upsilon(4S)$ resonance [8–10] and its uncertainty is between 12 and 30 deg, depending on the method [11]. This uncertainty is almost completely determined by the limited size of the data samples available, with theoretical uncertainties playing a negligible role ($\sim 1\%$). The large production of B mesons available at hadron colliders could offer a unique opportunity to improve the current experimental determination of the angle γ. However, the feasibility of this kind of measurement in

the larger background conditions of hadronic collisions has never been demonstrated.

In this paper we describe the first measurement of the branching fraction ratios and *CP* asymmetries of $B^{-} \to DK^{-}$ modes performed in hadron collisions, based on an integrated luminosity of 1 fb^{-1} of $\bar{p}p$ collisions at $\sqrt{s} = 1.96$ TeV collected by the upgraded Collider Detector (CDF II) at the Fermilab Tevatron. We reconstruct events where the D meson decays to the flavor-specific mode $K^{-}\pi^{+}$ (D_f^0), or to one of the *CP*-even modes $K^{-}K^{+}$ and $\pi^{-}\pi^{+}$ [$D_{CP+} = (D^0 + \bar{D}^0)/\sqrt{2}$]. From these modes, the following observables can be defined:

$$A_{CP+} = \frac{\mathcal{B}(B^{-} \to D_{CP+}K^{-}) - \mathcal{B}(B^{+} \to D_{CP+}K^{+})}{\mathcal{B}(B^{-} \to D_{CP+}K^{-}) + \mathcal{B}(B^{+} \to D_{CP+}K^{+})}, \tag{1}$$

$$R_{CP+} = 2\frac{\mathcal{B}(B^{-} \to D_{CP+}K^{-}) + \mathcal{B}(B^{+} \to D_{CP+}K^{+})}{\mathcal{B}(B^{-} \to D_f^0 K^{-}) + \mathcal{B}(B^{+} \to \bar{D}_f^0 K^{+})}. \tag{2}$$

With the assumption of no *CP* violation in D^0 decays, and neglecting D^0-$\bar{D}^0$ mixing [12], these quantities are related to the CKM angle γ by the equations [3]

$$R_{CP+} = 1 + r_B^2 + 2r\cos\delta_B\cos\gamma, \tag{3}$$

$$A_{CP+} = 2r_B \sin\delta_B \sin\gamma / R_{CP+}. \qquad (4)$$

For our measurements we adopt the usual approximation $R_{CP+} \sim \frac{R_+}{R}$, which is valid up to a term $r \cdot |V_{us}V_{cd}/V_{ud}V_{cs}| \simeq 0.01$ [13], where

$$R = \frac{\mathcal{B}(B^- \to D_f^0 K^-) + \mathcal{B}(B^+ \to \bar{D}_f^0 K^+)}{\mathcal{B}(B^- \to D_f^0 \pi^-) + \mathcal{B}(B^+ \to \bar{D}_f^0 \pi^+)}, \qquad (5)$$

$$R_+ = \frac{\mathcal{B}(B^- \to D_{CP+} K^-) + \mathcal{B}(B^+ \to D_{CP+} K^+)}{\mathcal{B}(B^- \to D_{CP+} \pi^-) + \mathcal{B}(B^+ \to D_{CP+} \pi^+)}. \qquad (6)$$

The CDF II detector is a multipurpose magnetic spectrometer surrounded by calorimeters and muon detectors. The components relevant for this analysis are briefly described here. A more detailed description can be found elsewhere [14]. Silicon microstrip detectors (SVX II and ISL) [15] and a cylindrical drift chamber (COT) [16] immersed in a 1.4 T solenoidal magnetic field allow reconstruction of charged particles in the pseudorapidity range $|\eta| < 1.0$ [17]. The SVX II detector consists of microstrip sensors arranged in five concentric layers with radii between 2.5 and 10.6 cm, divided into three contiguous sections along the beam direction z, for a total length of 90 cm. The two additional silicon layers of the ISL help to link tracks in the COT to hits in the SVX II. The COT has 96 measurement layers between 40 and 137 cm in radius, organized into alternating axial and $\pm 2°$ stereo superlayers, and provides a resolution on the transverse momentum of charged particles $\sigma_{p_T}/p_T \simeq 0.15\% p_T/(\text{GeV}/c)$. The specific energy loss by ionization (dE/dx) of charged particles in the COT can be measured from the collected charge, which is encoded in the output pulse width of each sense wire.

Candidate events for this analysis are selected by a three-level trigger system. At level 1, charged particles are reconstructed in the COT axial superlayers by a hardware processor, the extremely fast tracker (XFT) [18]. Two oppositely charged particles are required, with transverse momenta $p_T \geq 2$ GeV$/c$ and scalar sum $p_{T1} + p_{T2} \geq 5.5$ GeV$/c$. At level 2, the silicon vertex trigger (SVT) [19] associates SVX II $r - \phi$ position measurements with XFT tracks. This provides a precise measurement of the track impact parameter, d_0, which is defined as the distance of closest approach to the beam line. The resolution of the impact parameter measurement is 50 μm for particles with p_T of about 2 GeV$/c$, including a ≈ 30 μm contribution due to the transverse beam size, and improves for higher transverse momenta. We select B hadron candidates by requiring two SVT tracks with $120 \leq d_0 \leq 1000$ μm. To reduce background from light-quark jet pairs, the two trigger tracks are required to have an opening angle in the transverse plane $2° \leq \Delta\phi \leq 90°$, and to satisfy the requirement $L_{xy} > 200$ μm, where L_{xy} is defined as the distance in the transverse plane from the beam line to the two-track vertex, projected onto the two-track momentum

vector. The level 1 and 2 trigger requirements are then confirmed at trigger level 3, where the event is fully reconstructed.

Reconstruction of B^- hadrons begins by looking for a track pair that is compatible with a D^0 decay. The invariant mass (M_D) of the pair is required to be close to the nominal D^0 mass $(1.8 < M_D < 1.92$ GeV$/c^2)$. This is checked separately for each of the four possible mass assignments to the two outgoing particles: $K^+ \pi^-$, $K^- \pi^+$, $K^+ K^-$, and $\pi^+ \pi^-$. The D^0 candidate is combined with a negative charged track in the event with $p_T > 0.4$ GeV to form B^- candidates. A kinematic fit of the decay is performed by constraining the two tracks forming the D candidate to a common vertex and to the nominal D^0 mass, the D candidate and the remaining track to a separate vertex, and the reconstructed momentum of the B^- candidate to point back to the luminous region in the transverse plane.

To complete the selection, further requirements are applied on additional observables: the impact parameter (d_B) of the reconstructed B candidate relative to the beam line; the isolation of the B candidate (I_B) [20]; the goodness of fit of the decay vertex (χ_B^2); the transverse distance of the D, both relative to the beam $[L_{xy}(D)]$ and to the B vertex $[L_{xyB}(D)]$, and the significance of the B hadron decay length $[L_{xy}(B)/\sigma_{L_{xy}(B)}]$. We chose the requirement $L_{xyB}(D) > 100$ μm to reduce contamination from (nonresonant) three-body decays of the type $B^+ \to h^+ h^- h^+$ (from here on, we will use h to indicate either K or π), in which all tracks come from a common decay vertex. In addition, we reject all candidates comprising a pair of tracks with an invariant mass compatible with a $J/\psi \to \mu^+ \mu^-$ decay within 2σ. The threshold values for all other requirements, whose purpose is to reduce combinatorial background, were determined by an unbiased optimization procedure aimed at achieving the best resolution on A_{CP+}. This resolution was parametrized as a function of the expected signal yield S and background level B, by performing repeated fits on samples of simulated data extracted from the same multidimensional distribution used as likelihood function in the fit [Eq. (7)]. For each choice of thresholds, the signal S was determined by rescaling the number of observed $B^- \to D_f^0 \pi^-$, and the background B was determined from the upper mass sidebands of each data sample $(5.4 < M_B < 5.8$ GeV$/c^2)$. Based on this optimization procedure, we adopted the following set of requirements: $I_B > 0.65$, $\chi_B^2 < 13$, $d_B < 70$ μm, $L_{xy}(B)/\sigma_{L_{xy}(B)} > 12$, and $L_{xy}(D) > 400$ μm.

For every $B^- \to Dh^-$ candidate, a nominal invariant mass is evaluated by assigning the charged pion mass to the particle h^- coming from the B decay. The distributions obtained for the three modes of interest $(D \to K\pi, KK, $ or $\pi\pi)$ are reported in Fig. 1. A clear $B^- \to D\pi^-$ signal is seen in each. Events from $B^- \to DK^-$ decays are expected to form much smaller and wider peaks in these plots, located about 50 MeV$/c^2$ below the $B^- \to D\pi^-$ peaks,
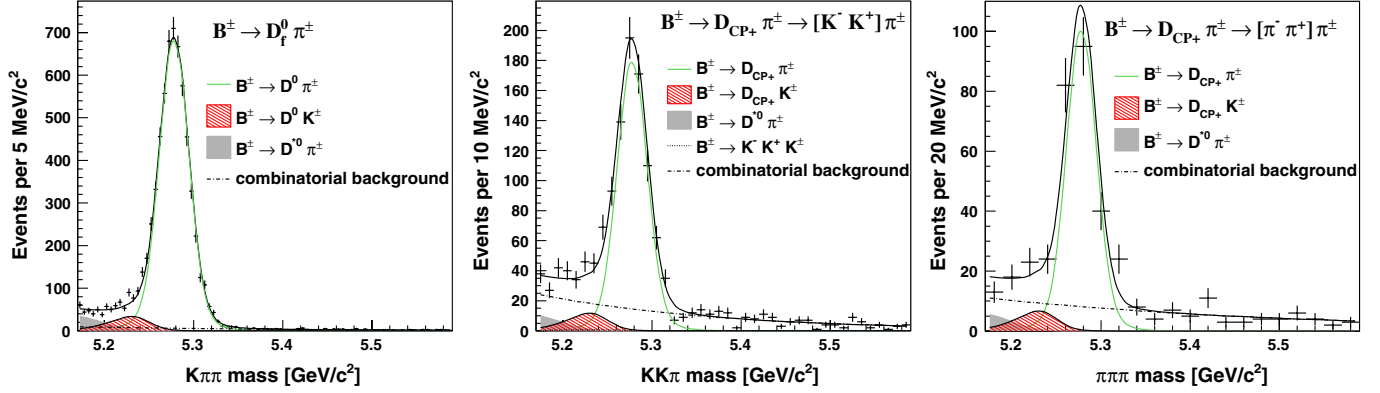
FIG. 1 (color online).   Invariant mass distributions of $B^- \to D\pi^-$ candidates for each reconstructed decay mode. The pion mass is assigned to the charged track from the B candidate decay vertex. The projections of the common likelihood fit (see text) are overlaid for each mode.

and as such cannot be resolved. The dominant residual backgrounds are random track combinations that meet the selection requirements (combinatorial background), misreconstructed physics background such as $B^- \to D^{*0}\pi^-$ decay, and, in the $D^0 \to KK$ final state, the non-resonant $B^- \to K^+K^-K^-$ decay, as determined by a study performed on CDF simulation.

We used an unbinned likelihood fit, exploiting kinematic and particle identification information from the measurement of dE/dx in a similar way to [21], to separate statistically the $B^- \to DK^-$ contributions from the $B^- \to D\pi^-$ signals and from the combinatorial background. To make best use of the available information, we fit the three modes simultaneously using a single likelihood function, to take advantage of the presence of parameters common to the three modes.

The likelihood function is

$$\mathcal{L} = \prod_i (1-b)\sum_j f_j \mathcal{L}_j^{\text{kin}} \mathcal{L}_j^{\text{PID}} + b \mathcal{L}_c^{\text{kin}} \mathcal{L}_c^{\text{PID}}, \quad (7)$$

where c labels combinatorial background quantities, b is the combinatorial background fraction, and $\mathcal{L}^{\text{kin}}$ and $\mathcal{L}^{\text{PID}}$ are defined below. The index j runs over the modes $B^- \to DK^-$, $B^- \to D\pi^-$, nonresonant $B^- \to K^+K^-K^-$ and $B^- \to \pi^+\pi^-K^-$, and $B^- \to D^{*0}\pi^-$ (where a soft γ or π^0 from the D^{*0} is undetected) and f_j are the fractions to be determined by the fit. The fraction of the physics background ($B^- \to D^{*0}\pi^-$) with respect to the signal is common to the three decays and the fraction of the $B^- \to D_{CP+}\pi^-$ is common to the two D_{CP} modes. As determined from simulation, these modes are the only significant contributions within the mass range $5.17 < M < 5.60$ GeV/c^2 chosen for our fit.

Kinematic information is given by three loosely correlated observables: (a) the mass $M_{D\pi}$, calculated by assigning the pion mass to the track from the B decay; (b) the momentum imbalance α, defined as

$$\alpha = 1 - p_{\text{tr}}/p_D > 0 \quad \text{if } p_{\text{tr}} < p_D;$$

$$\alpha = -(1 - p_D/p_{\text{tr}}) \leq 0 \quad \text{if } p_{\text{tr}} \geq p_D;$$

where p_{tr} is the momentum of the track from the B candidate; and (c) the scalar sum of the D momentum and the momentum of the track from the B candidate ($p_{\text{tot}} = p_{\text{tr}} + p_D$). The above variables uniquely identify the invariant mass M_{DK} evaluated with a kaon mass assignment to the track from the B decay, through the (exact) relations [22]

$$M_{DK}^2 = M_{D\pi}^2 + m_\pi^2 - m_K^2$$
$$+ 2\sqrt{m_D^2 + \frac{p_{\text{tot}}^2}{(2-\alpha)^2}}\left(\sqrt{m_\pi^2 + \left(\frac{p_{\text{tot}}(1-\alpha)}{2-\alpha}\right)^2}\right.$$
$$\left. - \sqrt{m_K^2 + \left(\frac{p_{\text{tot}}(1-\alpha)}{2-\alpha}\right)^2}\right),$$

if $\alpha > 0$;

$$M_{DK}^2 = M_{D\pi}^2 + m_\pi^2 - m_K^2$$
$$+ 2\sqrt{m_D^2 + \left(\frac{p_{\text{tot}}(1+\alpha)}{2+\alpha}\right)^2}\left(\sqrt{m_\pi^2 + \left(\frac{p_{\text{tot}}}{2+\alpha}\right)^2}\right.$$
$$\left. - \sqrt{m_K^2 + \left(\frac{p_{\text{tot}}}{2+\alpha}\right)^2}\right),$$

if $\alpha \leq 0$. Using these variables, we can write $\mathcal{L}_j^{\text{kin}} = P_j(M_{D\pi}|\alpha, p_{\text{tot}})P_j(\alpha, p_{\text{tot}})$ and $\mathcal{L}_j^{\text{PID}} = P_j(dE/dx|\alpha, p_{\text{tot}})$, where P_j is the probability density function for decay mode j. Distributions of the kinematic variables for the signals are obtained from samples of events from the full CDF simulation, while for the combinatorial background they are obtained from the mass sidebands of data. The shape of the mass distribution assigned to each signal process ($B^- \to D\pi^-$ and $B^- \to DK^-$ decays) has been modeled in detail from a dedicated study including the effect of final state QED radiation [23]. The simulation results were tested on high-statistics data

TABLE I. $B^- \to DK^-$ and $B^- \to D\pi^-$ event yields obtained from the fit to the data.

D mode	$B^+ \to D\pi^+$	$B^- \to D\pi^-$	$B^+ \to DK^+$	$B^- \to DK^-$	$B^+ \to [h^- h^+]K^+$	$B^- \to [h^- h^+]K^-$
$K^-\pi^+$	3769 ± 68	3763 ± 68	250 ± 26	266 ± 27		
K^+K^-	381 ± 25	399 ± 26	22 ± 8	49 ± 11	3 ± 1	3 ± 1
$\pi^+\pi^-$	101 ± 13	117 ± 14	6 ± 6	14 ± 6		

samples of D^0 decays, in order to ensure the reliability of the extraction of the DK^- component in the vicinity of the larger $D\pi^-$ peak. Exponential functions were used to model the mass distribution of combinatorial background for each mode. The normalization and the slope of these functions are independently determined in the maximum likelihood fit. The particle identification (PID) model of the combinatorial background allows for pion and kaon components, which are free to vary in the fit.

A large sample of $D^{*+} \to D^0(\to K^-\pi^+)\pi^+$ decays was used to calibrate the dE/dx response of the detector to kaons and pions, using the charge of the pion in the D^{*+} decay to determine the identity of the D^0 decay products. The calibration includes the dependence of the shape and the average of the response curve on particle momentum, and the shape of the distribution of common-mode fluctuations. The calibrated dE/dx information provides a 1.5σ separation power between pion and kaon particles of $p_T > 2$ GeV/c. Uncertainties on the calibration parameters are included in the final systematic uncertainty of A_{CP+} and R_{CP+} [22].

The $B^- \to DK^-$ and $B^- \to D\pi^-$ signal event yields obtained from the fit to the data are reported in Table I. The fraction of the $B^- \to \pi^+\pi^-K^-$ was set by the fit to its lower bound at zero, compatible with the expectation of a negligible contribution, and will be ignored in the following. The uncorrected values of the double ratio of branching fractions R_{CP+} and of the CP asymmetry A_{CP+} obtained from the fit are $R_{CP+} = 1.27 \pm 0.24$ and $A_{CP+} = 0.39 \pm 0.17$. In the fit, R_{CP+} and A_{CP+} are functions of the

fractions [f_j in Eq. (7)] and the total number of events in each subsample.

As a check of the goodness of the fit, and to visualize better the separation between signal and background, we plot distributions of the relative signal likelihoods:

$$RL = \frac{\text{pdf}(B \to DK)}{\text{pdf}(B \to DK) + \text{pdf(background)}} \quad (8)$$

where pdf$(B \to DK)$ is the probability density under the signal hypothesis, and pdf (background) is the probability density under the background hypothesis (including both physics and combinatorial backgrounds, with their measured relative fractions). These distributions are compared to the prediction of our fit in Fig. 2, showing a very good agreement. In addition, we plot projections of the fit on the invariant mass distributions, both for the entire sample (Fig. 1), and for a kaon-enriched subsample, where the interesting $B^- \to DK^-$ components have been enhanced with respect to the $B^- \to D\pi^-$ by means of a dE/dx cut (Fig. 3). All these projections show very good agreement between our fit and the data.

Some corrections are needed to convert our fit results into measurements of the parameters of interest. First, we correct for small biases in the fit procedure itself, as measured by repeated fits on simulated samples: $\delta(R_{CP+}) = -0.027 \pm 0.005$ and $\delta(A_{CP+}) = 0.015 \pm 0.003$. These biases are independent of the true values of A_{CP+} and R_{CP+} used in the simulated samples. R_{CP+} does not need any further corrections because detector effects
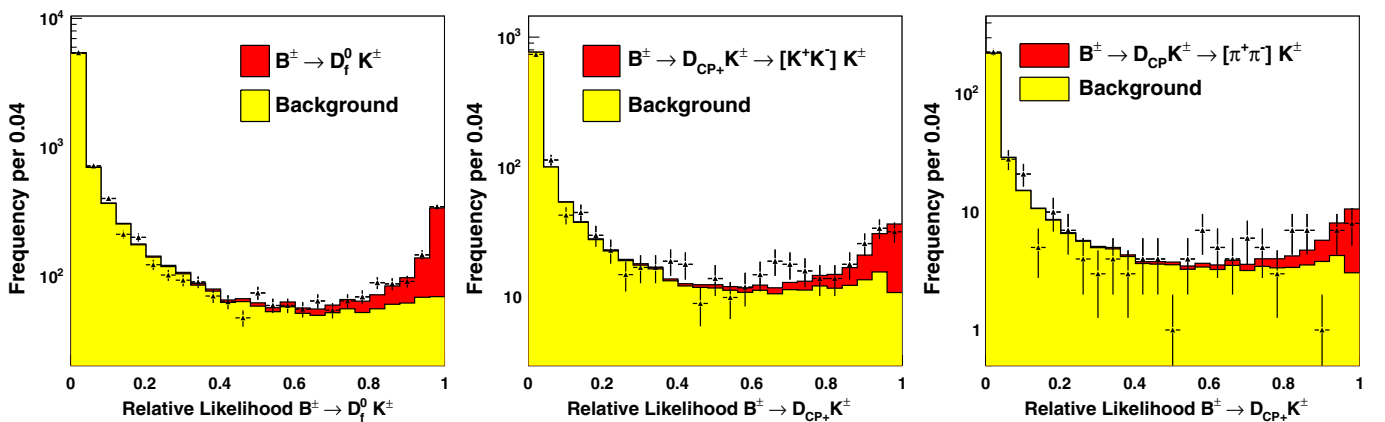

FIG. 2 (color online).   Relative likelihood for $B^- \to DK^-$ candidates for each reconstructed decay mode. The points with the error bars show the distribution obtained on the fitted data sample while the histograms show the distributions obtained by generating signal and background events directly from the total probability distribution function (pdf) of the fit composition.
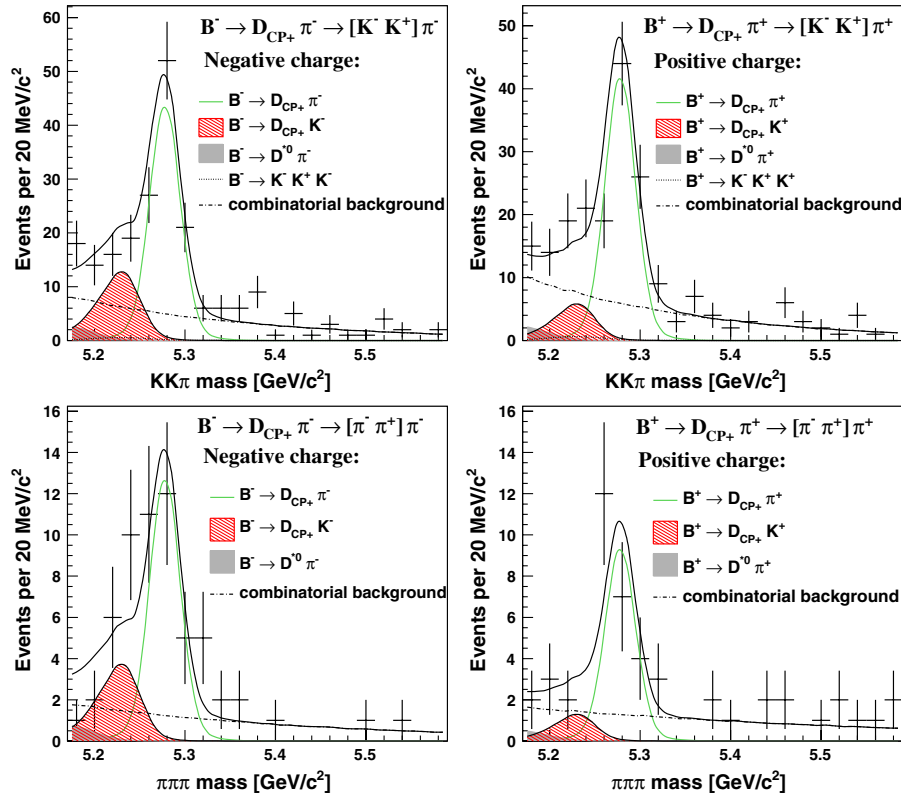
FIG. 3 (color online). Invariant mass distributions of $B^- \to D\pi^-$ candidates for each reconstructed decay mode. The pion mass is assigned to the prompt track from the B decay. A requirement on the PID variable was applied to suppress the $D\pi$ component and favor the DK component. The projections of the likelihood fit for each mode are overlaid. The p value for agreement of data with the fit is 0.95

cancel in the double ratio of branching fractions. The direct CP asymmetry A_{CP+} needs to be corrected for the different probability for K^+ and K^- mesons to interact with the tracker material. This effect is reproduced well by CDF II detector simulation (traced by GEANT [24]), which yields an estimate $\frac{\epsilon(K^+)}{\epsilon(K^-)} = 1.0178 \pm 0.0023(\text{stat}) \pm 0.0045(\text{syst})$ [25] which has been verified by measurements on data [26].

The corrected results are

$$R_{CP+} = 1.30 \pm 0.24(\text{stat}), \qquad (9)$$

$$A_{CP+} = 0.39 \pm 0.17(\text{stat}), \qquad (10)$$

where A_{CP+} was corrected using the following equation:

$$A_{CP+} = \frac{N(B^- \to D^0_{CP+}K^-)\frac{\epsilon(K^+)}{\epsilon(K^-)} - N(B^+ \to D^0_{CP+}K^+)}{N(B^- \to D^0_{CP+}K^-)\frac{\epsilon(K^+)}{\epsilon(K^-)} + N(B^+ \to D^0_{CP+}K^+)}. \qquad (11)$$

Systematic uncertainties are listed in Table II. They were determined by generating simulated samples of pseudoexperiments with different underlying assumptions, and checking the effect of such changes on the results of our measurement procedure. The dominant contributions are uncertainty on the dE/dx calibration and parametrization, uncertainty on the kinematics of the combinatorial background, and uncertainty on the physics background ($B^- \to D^{*0}\pi^-$) mass distribution. Variations in the model of the combinatorial background included different functional forms of the mass distribution, and alternative (α, p_{tot}) distributions, constrained by comparison with real data in the mass sidebands.

TABLE II. Summary of systematic uncertainties.

Source	R_{CP+}	A_{CP+}
dE/dx model	0.056	0.030
$D^{*0}\pi$ mass model	0.025	0.006
Input B^- mass to the fit	0.004	0.002
Combinatorial background mass model	0.020	0.001
Combinatorial background kinematics	0.100	0.020
$D\pi$ kinematics	0.002	0.001
DK kinematics	0.002	0.004
$D^{*0}\pi$ kinematics	0.004	0.002
Fit bias	0.005	0.003
Total (sum in quadrature)	0.12	0.04

Smaller contributions are assigned for trigger efficiencies, assumed B^- mass input in the fit [27], and kinematic properties of signal and physics background.

In summary, we have measured the double ratio of CP-even to flavor eigenstate branching fractions [Eq. (2)] $R_{CP+} = 1.30 \pm 0.24(\text{stat}) \pm 0.12(\text{syst})$ and the direct CP asymmetry [Eq. (1)] $A_{CP+} = 0.39 \pm 0.17(\text{stat}) \pm 0.04(\text{syst})$. These results can be combined with other $B^- \rightarrow DK^-$ decay parameters to improve the determination of the CKM angle γ. These measurements are performed here for the first time in hadron collisions, are in agreement with previous measurements from *BaBar* ($R_{CP+} = 1.06 \pm 0.10 \pm 0.05$, $A_{CP+} = 0.27 \pm 0.09 \pm 0.04$ in 348 fb^{-1} of integrated luminosity [9]) and Belle ($R_{CP+} = 1.13 \pm 0.16 \pm 0.08$, $A_{CP+} = 0.06 \pm 0.14 \pm 0.05$ in 250 fb^{-1} of integrated luminosity [10]) and have comparable uncertainties.

We thank the Fermilab staff and the technical staffs of the participating institutions for their vital contributions.

[1] The charge conjugate state is implied throughout the paper, except in formulas and sentences where both are mentioned explicitly.

[2] M. Kobayashi and T. Maskawa, Prog. Theor. Phys. **49**, 652 (1973); N. Cabibbo, Phys. Rev. Lett. **10**, 531 (1963).

[3] M. Gronau and D. Wyler, Phys. Lett. B **265**, 172 (1991); M. Gronau and D. London, Phys. Lett. B **253**, 483 (1991).

[4] D. Atwood, I. Dunietz, and A. Soni, Phys. Rev. D **63**, 036005 (2001); Phys. Rev. Lett. **78**, 3257 (1997).

[5] A. Giri, Y. Grossman, A. Soffer, and J. Zupan, Phys. Rev. D **68**, 054018 (2003).

[6] R. Fleischer, Phys. Lett. B **459**, 306 (1999); R. Fleischer and J. Matias, Phys. Rev. D **66**, 054009 (2002).

[7] I. Dunietz, R. Fleischer, and U. Nierste, Phys. Rev. D **63**, 114015 (2001).

[8] E. Barberio *et al.* (Heavy Flavor Averaging Group (HFAG)), arXiv:hep-ex/0808.1297v3.

[9] B. Aubert *et al.* (*BABAR* Collaboration), Phys. Rev. D **77**, 111102 (2008).

[10] K. Abe *et al.* (BELLE Collaboration), Phys. Rev. D **73**, 051106 (2006).

[11] J. Charles *et al.* (CKMfitter Group) Eur. Phys. J. C **41**, 1 (2005), updated results and plots available at http://ckmfitter.in2p3.fr; M. Bona *et al.* (UTfit Collaboration) J. High Energy Phys. 10 (2006) 081, updated results and plots available at http://www.utfit.org/.

[12] Y. Grossman, A. Soffer, and J. Zupan, Phys. Rev. D **72**, 031501(R) (2005).

[13] M. Gronau, Phys. Lett. B **557**, 198 (2003); Phys. Rev. D **58**, 037301 (1998).

[14] D. E. Acosta *et al.* (CDF Collaboration), Phys. Rev. D **71**, 032001 (2005).

[15] A. Sill, Nucl. Instrum. Methods Phys. Res., Sect. A **447**, 1

[16] A. Affolder *et al.*, Nucl. Instrum. Methods Phys. Res., Sect. A **526**, 249 (2004).

[17] CDF II uses a cylindrical coordinate system in which ϕ is the azimuthal angle, r is the radius from the nominal beam line, and z points in the proton beam direction, with the origin at the center of the detector. The transverse plane is the plane perpendicular to the z axis.

[18] E. J. Thomson *et al.*, IEEE Trans. Nucl. Sci. **49**, 1063 (2002).

[19] B. Ashmanskas *et al.*, Nucl. Instrum. Methods Phys. Res., Sect. A **518**, 532 (2004).

[20] Isolation is defined as $I_B = p_T(B)/(p_T(B) + \sum_i p_{Ti})$, where $p_T(B)$ is the transverse momentum of the B candidate, and the sum runs over all other tracks within a cone of radius 1, in $\eta - \phi$ space around the B flight direction. Its value is typically higher for bottom-flavored hadrons than for random track combinations.

[21] A. Abulencia *et al.* (CDF Collaboration), Phys. Rev. Lett. **97**, 211802 (2006).

[22] P. Squillacioti, Ph.D. thesis, University of Siena [Report No. FERMILAB-THESIS-2006-27, 2006].

[23] T. Aaltonen *et al.* (CDF Collaboration), Phys. Rev. Lett. **103**, 031801 (2009).

[24] R. Brun, R. Hagelberg, M. Hansroul, and J. C. Lasalle, Reports No. CERN-DD-78-2-REV and No. CERN-DD-78-2.

[25] D. E. Acosta *et al.* (CDF Collaboration), Phys. Rev. Lett. **94**, 122001 (2005).

[26] M. Morello (CDF Collaboration), Nucl. Phys. B, Proc. Suppl. **170**, 39 (2007).

[27] D. E. Acosta *et al.* (CDF Collaboration), Phys. Rev. Lett. **96**, 202001 (2006).

(2000).